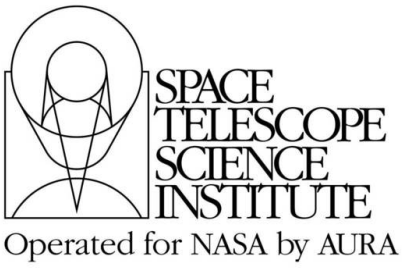

Bayesian system identification and predictive algorithms for exoplanet imaging

Supervised by :

Laurent Pueyo & Colin Norman

Théo Jolivet

July 2020

Abstract

The main limitation for achieving observations in direct high-contrast imaging is the low information regime we are in because the space telescope is photon-starved. In such a case, the residual electric field from the host star is predominant in the face of the electric field from the planet we are interested in. Wavefront Sensing and Control (WFS&C) are methods using both estimation and control algorithms to correct errors in the telescope's optics and allow to observe planets much fainter than their host stars in the search for life. Until now, no space telescope has integrated WFS&C algorithms but they could greatly enhance the image processing contrast. In current designs, previous information is discarded at each step of estimation and control. We demonstrate that it is beneficial to account for past history of photons on the science camera and propose a prediction framework that significantly reduces the instrument observation time. The algorithm has been validated in both simulation and in experimentation. We show that it divides the estimation time by a factor 5 while being resilient to drift and misalignments. An article is in preparation and a version of this algorithm could one day be implemented on NASA's Large Ultraviolet/Optical/Infrared Surveyor (LUVOIR) mission.

Contents

1 Introduction

The great challenge in future NASA flagship missions is the direct imaging and characterization of exoplanets in the search for life [6] [7]. The difficulty is that those exoplanets orbit around a star that is much brighter than them. There remains an important residual electric field (speckles) from the star on the science camera, which prevents us from achieving sufficient contrast to observe planets that are 10^{10} times fainter than their host star. In what follows, the *planet* refers to the object we want to characterize, the *star* refers to a much brighter object near it and *speckles* refers to the residual electric field from the star on the science camera.

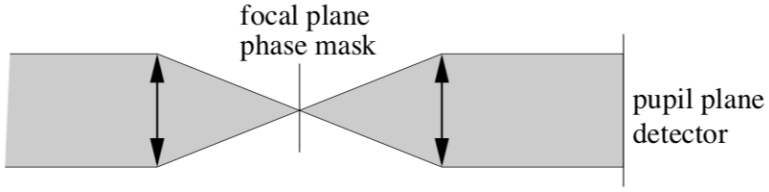

Figure 1: Simplified optical representation of a coronagraph, the focal plane mask is designed to block the light from the star.

Direct imaging of exoplanets is allowed by a specifically designed instrument called a coronagraph seen on Fig. (1), which produces destructive interferences to suppress starlight. The random nature of starlight implies a residual electric field that also needs to be adressed so it can also be nullified by the coronagraph, which is why we need deformable mirrors (DMs) to estimate and control the speckles. This technology has never been sent to space yet and is essential in WFS&C. Such a configuration allows for a much greater contrast compared to present methods, but it needs a significantly better wavefront estimation precision. The system is consequently corrected in closed-loop using WFS&C algorithms that create a zone where the contrast is very important in the image camera plane thanks to small actuations (dithering) of the DMs.

Fig. (2) shows the relative intensity of the speckles at the science camera with and without DMs control. On the right-hand side, we achieved a "dark hole", zone of great contrast that would potentially allow to see very dim exoplanets. Note that when refering to an "important" contrast, we are talking about a small intensity of the speckles. The more we *reduce the*

intensity, *i.e.* going from 10^{-5} to 10^{-7} for example, the more we *increase the contrast*. Formally, the contrast is the intensity of the corrected image divided by the intensity of the image that avoids the coronagraph.

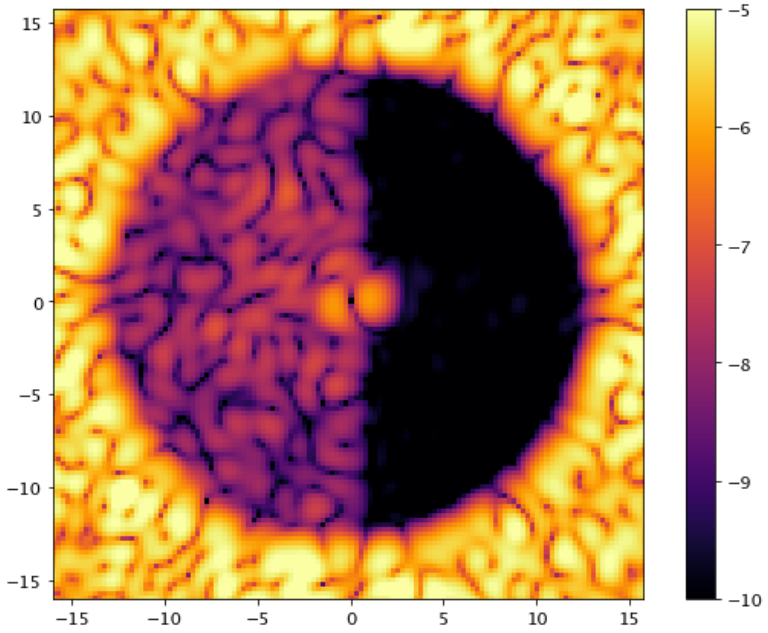

Figure 2: Intensity of the speckles in the camera plane with (right) and without (left) correction, contrast in log-scale is shown. The dark hole is the black half-circle with important contrast.

We showed that we can improve WFS&C algorithms by using statistical methods that have not been explored in this field. We implemented a predictive algorithm based on Empirical Orthogonal Functions (EOFs) that filters the history of previous information to gain significant time in the estimation step while being robust to noise. This algorithm would be used for "dark hole maintenance", that is to say when we have already reached a zone of important contrast.

This paper is organized as follows. First, in Section 2 we describe the model of the considered optical system of the telescope and present the main assumptions about the instrument. In Section 3, we introduce the principal estimation and control algorithms for WFS&C. In Section 4, we propose a framework for prediction and we compare the numerical results of our algorithm to state-of-the-art methods in Section 5. Finally, we conclude our work in Section 6 and suggest possible developments.

2 Overview of the Optical System of a Space Telescope

In this section, we introduce the main optical elements of the telescope and develop the equations that lead to the general linear model of the system.

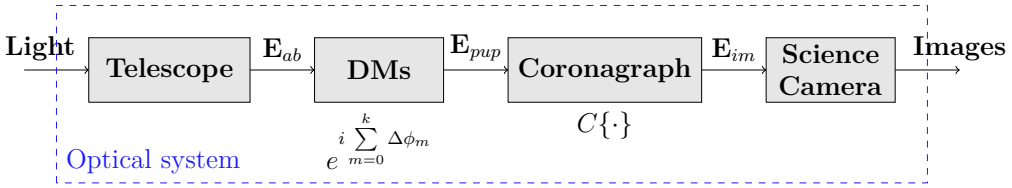

Figure 3: Block diagram of the optical correction system comprised of the coronagraph and the deformable mirrors. The coronagraph is a series of masks, lenses, and free space propagation between the pupil (DM) plane and the focal (camera) plane.

As seen in Fig. (3), the light enters the telescope, then its aberrated electric field $\mathbf{E}_{ab}$ undergoes two important transformations. First, the DMs introduce *phase* perturbation at the pupil plane. Then, this field travels through the coronagraph, which is a *linear* transformation at the image plane denoted $C\{\cdot\}$. The science camera measures the intensity of the electric field and other incoherent light at the focal plane.

Remark. *Boldface characters such as* $\mathbf{E}_{im}$ *denote the complex electric field on each pixel of the science camera, and can be both defined in matrix or vector form. In this section, we will start from a matrix representation where the position is denoted by* (x, y) *then derive a vector form. This naturally comes from the fact that this is what is done in practice when we implement the algorithms later described.*

To be coherent with our numerical implementations, we follow the convention where the numeration *starts at zero*. Consequently, $\mathbf{E}_{im,0}$ is the electric field at the science camera after the first correction step.

Without loss of generality, we consider a system with only one DM where the phase correction at each control step is a small deviation from the one at the previous step. For instance at pixel (x, y), it is $\Delta\phi_0(x, y) + \Delta\phi_1(x, y) + \Delta\phi_2(x, y)$ after the third step. After correction step $k + 1$, the electric field at pixel (x, y) of the image plane is then:

$$
\begin{aligned}
E_{im,k}(x,y) &= C\{E_{pup,k}(x,y)\} \\
&= C\{E_{ab}(x,y)e^{\,i\sum_{m=0}^{k}\Delta\phi_m(x,y)}\} \\
&= C\{E_{ab}(x,y)e^{\,i\sum_{m=0}^{k-1}\Delta\phi_m(x,y)}(1+(e^{i\Delta\phi_k(x,y)}-1))\} \\
&= \underbrace{C\{E_{ab}(x,y)e^{\,i\sum_{m=0}^{k-1}\Delta\phi_m(x,y)}\}}_{E_{im,k-1}(x,y)} + C\{E_{ab}(x,y)e^{\,i\sum_{m=0}^{k-1}\Delta\phi_m(x,y)}(e^{i\Delta\phi_k(x,y)}-1)\}
\end{aligned}
\tag{1}
$$

Assuming $\Delta\phi_k$ is very small, we take the first-order Taylor expansion of the exponential and rewrite the electric field at step $k+1$ as a sum of the electric field at step k and the influence of DMs at step $k+1$:

$$
E_{im,k}(x,y) = E_{im,k-1}(x,y) + C\{E_{ab}(x,y)e^{\,i\sum_{m=0}^{k-1}\Delta\phi_m(x,y)} i\Delta\phi_k(x,y)\} \tag{2}
$$

We then rewrite the DMs phase deviation in terms of their voltage commands $\mathbf{u}_k = [u_{0,k},\ u_{1,k},\ \cdots,\ u_{N_{act}-1,k}]^T$, assuming that the total effect of the DMs is the sum of individual influence functions f_q from the N_{act} degrees of freedom. Here, $(\cdot)^T$ denotes the vector transpose and $f_q : \mathbb{R}^{N_{pix}} \to \mathbb{R}$ the function that represents the effect of the q^{th} actuator at every pixel of the science camera. On the testbed, $N_{act} = 34 \times 34$, and it is expected to be of the same order on the real telescope.

$$
\Delta\phi_k(x,y) = \Delta\phi(\mathbf{u}_k, x, y) = \sum_{q=0}^{N_{act}-1} u_{q,k} f_q(x,y) \tag{3}
$$

This linearity assumption is the reference for the optical system modelling in the community [2], and finding ways of tracking the non-linearities in the system could be an axis of research for the rest of the internship.

Substituting Eq. (3) in Eq. (2) and using the linearity property of $C\{\cdot\}$ we get:

$$
E_{im,k}(x,y) = E_{im,k-1}(x,y) + \sum_{q=0}^{N_{act}-1} C\{iE_{ab}(x,y)e^{\,i\sum_{m=0}^{k-1}\Delta\phi_m(x,y)} f_q(x,y)\}\ u_{q,k} \tag{4}
$$

Concatenating on all N_{pix} pixels following the process in Appendix A, Eq. (4) can be simplified in vector form as

$$\mathbf{E}_{im,k} = \mathbf{E}_{im,k-1} + \mathbf{G}_k \mathbf{u}_k \tag{5}$$

With $\mathbf{E}_{im,k} \in \mathbb{R}^{N_{pix}}$ the electric field vector on the science camera, $\mathbf{u}_k \in \mathbb{R}^{N_{act}}$ the vector of DMs actuations at step $k+1$. $\mathbf{G}_k \in \mathbb{R}^{N_{pix} \times N_{act}}$ is the Jacobian matrix, formally written as

$$\mathbf{G}_k = (g_{y,z}) \begin{array}{l} 0 \leq y < N_{pix} \\ 0 \leq z < N_{act} \end{array} \coloneqq C\{iE_{ab}(y) e^{i \sum_{m=0}^{k-1} \Delta\phi_m(y)} f_z(y)\} \tag{6}$$

Such that the $(y,z)^{th}$ entry of $\mathbf{G}_k$ represents the influence of the z^{th} actuator on the y^{th} pixel. $\mathbf{G}_k$ is calculated by propagating each influence function through the coronagraph separately.

Remark. *We established in this section a vector form of the electric field. From now on, objects of the form* $\mathbf{E}_{im}$ *will denote vectors.*

3 Estimation and Control Algorithms for WFS&C

In the following section, we present the most popular algorithms for estimation and control using the linearized approximation Eq.(2). More discussion on these methods can be found in [2].

WFS&C algorithms are comprised of two steps: an estimation step and a control step in closed-loop, see Fig. (4). To reduce the speckles field in closed-loop, we must first estimate it. The goal is to estimate the electric field given its intensity on the science camera in order to choose the DMs actuations that minimize it in the control step.

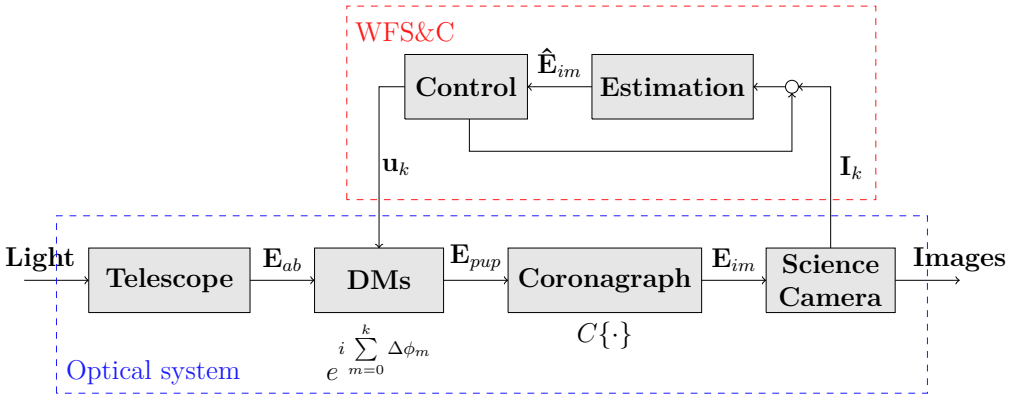

Figure 4: Block diagram of the estimation and control closed-loop.

3.1 Estimation: Pairwise Probe Estimator

The most common estimator is the pairwise probe estimator. It uses small actuations (dithering) of the DMs to probe the electric field. By adding and subtracting such commands to the electric field, one is able to give its best estimate in the least squares sense. We aim at estimating $\mathbf{E}_{im,k-1}$ by choosing a set of known s probe functions $\mathbf{u}^p = [u_0^p,\ u_1^p,\ \cdots,\ u_{s-1}^p]^T$.

By alternating them and applying them to the unknown electric field, we measure $\forall j \in (0, \cdots, s-1)$

$$\begin{aligned}
\mathbf{I}_j^+ &= |\mathbf{E}_{im,k-1} + \mathbf{G}_k \mathbf{u}_j^p|^2 \\
&= |\mathbf{E}_{im,k-1}|^2 + |\mathbf{G}_k \mathbf{u}_j^p|^2 + 2\mathrm{Re}(\bar{\mathbf{E}}_{im,k-1} \circ \mathbf{G}_k \mathbf{u}_j^p) \\
\mathbf{I}_j^- &= |\mathbf{E}_{im,k-1} - \mathbf{G}_k \mathbf{u}_j^p|^2 \\
&= |\mathbf{E}_{im,k-1}|^2 + |\mathbf{G}_k \mathbf{u}_j^p|^2 - 2\mathrm{Re}(\bar{\mathbf{E}}_{im,k-1} \circ \mathbf{G}_k \mathbf{u}_j^p)
\end{aligned} \tag{7}$$

Where $\circ$ denotes element-wise product and $\bar{\mathbf{E}}$ is the vector of each conjugate element of $\mathbf{E}$. We then subtract those two equations to get

$$\mathbf{I}_j^+ - \mathbf{I}_j^- = 4\mathrm{Re}(\bar{\mathbf{E}}_{im,k-1} \circ \mathbf{G}_k \mathbf{u}_j^p), \ \forall j \in (0, \cdots, s-1) \tag{8}$$

We remind the identity $\mathrm{Re}(\bar{\mathbf{a}} \circ \mathbf{b}) = \mathrm{Re}(\mathbf{a}) \circ \mathrm{Re}(\mathbf{b}) + \mathrm{Im}(\mathbf{a}) \circ \mathrm{Im}(\mathbf{b})$, where $\mathbf{a}$ and $\mathbf{b}$ are two complex vectors of the same size and the Real and Imaginary operators are applied element-wise. Eq. (8) at pixel $m+1$ then becomes:

$$\begin{aligned}
[\mathbf{I}_j^+ - \mathbf{I}_j^-]_m &= 4([\mathrm{Re}(\mathbf{E}_{im,k-1})]_m [\mathrm{Re}(\mathbf{G}_k \mathbf{u}_j^p)]_m + [\mathrm{Im}(\mathbf{E}_{im,k-1})]_m [\mathrm{Im}(\mathbf{G}_k \mathbf{u}_j^p)]_m) \\
&= 4 \begin{pmatrix} [\mathrm{Re}(\mathbf{G}_k \mathbf{u}_j^p)]_m & [\mathrm{Im}(\mathbf{G}_k \mathbf{u}_j^p)]_m \end{pmatrix} \begin{pmatrix} [\mathrm{Re}(\mathbf{E}_{im,k-1})]_m & [\mathrm{Im}(\mathbf{E}_{im,k-1})]_m \end{pmatrix}^T
\end{aligned} \tag{9}$$

Taking $s \geq 2$ probe pairs at pixel $m+1$, we form the system of equations

$$\begin{pmatrix} [\mathbf{I}_0^+ - \mathbf{I}_0^-]_m \\ \vdots \\ [\mathbf{I}_{s-1}^+ - \mathbf{I}_{s-1}^-]_m \end{pmatrix} = 4 \underbrace{\begin{pmatrix} [\mathrm{Re}(\mathbf{G}_k \mathbf{u}_0^p)]_m & [\mathrm{Im}(\mathbf{G}_k \mathbf{u}_0^p)]_m) \\ \vdots & \vdots \\ [\mathrm{Re}(\mathbf{G}_k \mathbf{u}_{s-1}^p)]_m & [\mathrm{Im}(\mathbf{G}_k \mathbf{u}_{s-1}^p)]_m) \end{pmatrix}}_{\mathbf{P}} \begin{pmatrix} [\mathrm{Re}(\mathbf{E}_{im,k-1})]_m \\ \\ [\mathrm{Im}(\mathbf{E}_{im,k-1})]_m \end{pmatrix} \tag{10}$$

We then take the pseudo-invert of the matrix $\mathbf{P}$ to obtain $\mathbf{E}_{im,k-1}$ at pixel $m+1$. This method is inefficient because we have to repeat this process for every $0 \leq m < N_{pix}$, and we do not account for previous values of $\mathbf{E}_{im}$. We introduce in Section 4 an estimation algorithm that solves this issue.

3.2 Control: Stroke Minimization and Electric Field Conjugation

Using the estimate of the electric field established with the algorithm presented in Subsection 3.1, we aim at minimizing the speckle field at the image plane.

Stroke minimization (SM) has been introduced in Pueyo et al. 2009 [8]. The goal is to find the smallest DMs command to achieve a given contrast.

$$\begin{array}{ll} \min\limits_{\mathbf{u}_k} & ||\mathbf{u}_k||_2^2 \\ \text{s.t.} & \mathbf{I}_{DH,k} = |\mathbf{E}_{DH,k}|^2 \leq C_k \end{array} \tag{11}$$

With C_k the contrast constraint that decreases each iteration and $\mathbf{I}_{DH}$ the total intensity inside of the dark hole. Finding the Lagrange constant is nontrivial and is done with a line search. The inequality is rewrote as an equality and the problem is reformulated with a Lagrange constant $\mu_k > 0$

$$\min_{\mathbf{u}_k} \mathbf{u}_k^T \mathbf{u}_k + \mu_k(\mathbf{E}_{DH,k}^\dagger \mathbf{E}_{DH,k} - C_k) = \mathbf{J}_k \tag{12}$$

Whereas Electric field conjugation (EFC) seeks to minimize the contrast with a Tikhonov regularization of the DMs actuation [1]

$$\begin{array}{ll} & \min\limits_{\mathbf{u}_k} |\mathbf{E}_{DH,k}|^2 + \lambda_k ||\mathbf{u}_k||_2^2 \\ \Leftrightarrow & \min\limits_{\mathbf{u}_k} (\mathbf{E}_{DH,k-1} + \mathbf{G}_k \mathbf{u}_k)^\dagger (\mathbf{E}_{DH,k-1} + \mathbf{G}_k \mathbf{u}_k) + \lambda_k ||\mathbf{u}_k||_2^2 = \mathbf{J}_k \end{array} \tag{13}$$

with $\lambda > 0$ the regularization parameter.

Setting to 0 the derivative of $\mathbf{J}_k$ with respect to $\mathbf{u}_k$ in Eq. (12) leads to

$$\begin{aligned} \frac{\partial \mathbf{J}_k}{\partial \mathbf{u}_k} = \frac{\partial \mathbf{u}_k^T \mathbf{u}_k + \mu_k((\mathbf{E}_{DH,k-1} + \mathbf{G}_k \mathbf{u}_k)^\dagger (\mathbf{E}_{DH,k-1} + \mathbf{G}_k \mathbf{u}_k) - C_k)}{\partial \mathbf{u}_k} &= \mathbf{0} \\ \Leftrightarrow 2\mathbf{u}_k + 2\mu_k(\mathbf{G}_k^\dagger \mathbf{E}_{DH,k-1} + \mathbf{G}_k^\dagger \mathbf{G}_k \mathbf{u}_k) &= \mathbf{0} \end{aligned}$$

which gives, if $(\mathbf{G}_k^\dagger \mathbf{G}_k + \frac{1}{\mu_k} \mathbb{I}_{N_{act}})$ is nonsingular

$$\mathbf{u}_k = -(\mathbf{G}_k^\dagger \mathbf{G}_k + \frac{1}{\mu_k} \mathbb{I}_{N_{act}})^{-1} \mathbf{G}_k^\dagger \mathbf{E}_{DH,k-1} \tag{14}$$

And gives the control law for the DMs actuation commands for the next correction step. Similarly, taking the derivative of the cost function in Eq. (13) with respect to $\mathbf{u}_k$ and setting it to 0 gives

$$\mathbf{u}_k = -(\mathbf{G}_k^\dagger \mathbf{G}_k + \lambda_k \mathbb{I}_{N_{act}})^{-1} \mathbf{G}_k^\dagger \mathbf{E}_{DH,k-1} \tag{15}$$

where $\mathbb{I}_{N_{act}}$ is the identity matrix of N_{act}.

We can see that both algorithms lead to the same law of command, the only difference being in the tuning parameters. Both λ_k and μ_k introduce a

damping term which prevents an ill-posed problem. Finding the right value for them turns out to be nontrivial and is the key to properly implementing the controllers.

4 Model-Free Predictive Algorithm for Estimation

We give in this section an overview of the Empirical Orthogonal Functions (EOFs), and derive their main properties from equations. We explain why they are useful in our case and give a sense of which challenges we expected to face when implementing them.

4.1 Motivation for Empirical Orthogonal Functions

EOFs were initially developed to counteract the time lag in ground telescopes due to the delay between wavefront estimation and effective correction. Indeed, the control loop on Fig. (4) is not instantaneous, so the field that ends up being corrected is no longer the same than the one that was estimated because of the speckles drift. It was crucial to introduce a way to predict which field we wanted to correct accounting for the time lag in the control loop. For that purpose, the EOFs framework has been introduced by Guyon and Males in [3] and presents several specificities that could help improving WFS&C methods.

Imagine the scenario where we don't account for time lag. We estimate an electric field $\mathbf{E}_{im}(t)$, then correct for it. But the control loop takes a time δt to process the next DMs actuation and we end up correcting for $\mathbf{E}_{im}(t)$, while the actual electric field is now $\mathbf{E}_{im}(t+\delta t)$. To counteract that, one can introduce a prediction step to feed $\mathbf{E}_{im}(t+\delta t)$ to the control loop, so that it will indeed correct for the present electric field. This point is particularly important for ground telescopes, where the control must be done at a kilohertz rate due to the atmospheric turbulence and this is for that pupose that EOFs have been used historically.

By going to space, we get rid of the atmospheric turbulence but we are now imaging much fainter planets, for which we have very little light coming from. This leads to an important integration time to collect enough photons on the science camera to produce just one image. We then forget every past information, repeat that process from scratch to obtain a second image and the total exposure time ends up taking hours for a single planet. We propose a scheme based on EOFs that allows to estimate an image at every step using previous information on the science camera.

In most algorithms for WFS&C, previous information about the speckles

is discarded. Instead, we store it to train a filter that gives an estimate of the future state. The latter is a linear combination of previous steps, and does not require a model for the data. Because of the Singular Value Decomposition (SVD) in the computing of the filter, we can incorporate other measurements such as the DMs actuation. Any addition that does not bring any information is automatically discarded by the SVD due to lack of correlation.

The practical implementation on a space telecope would result in an immense gain in operating time. Currently, we need to integrate $t = 0,\ 1,\ \cdots,\ T$ time frames to obtain an image. By stocking previous time frames, we are able to predict the next image, see Fig. (5). We would then have T images in T time frames instead of only one image like it is currently the case.

Overview The advantages of EOFs are multiple:

- EOFs are derived from least squares and we show in Subsection 4.2 that they converge to the **global optimal linear predictive controller**.
- **Model-free**. They don't need a model of the data, so one can use any representation of the images.
- They allow for **sensor fusion**, one can feed the algorithm with measurements from different sensors (DMs actuation and electric field for instance). Additions that don't bring any information are automatically discarded due to the lack of correlation in the SVD.
- The only computationally expensive part is the SVD and it is independant of which quantity we want to estimate. Thus once it is computed, it is possible to estimate the wavefront **at every pixel** at very low additional cost.

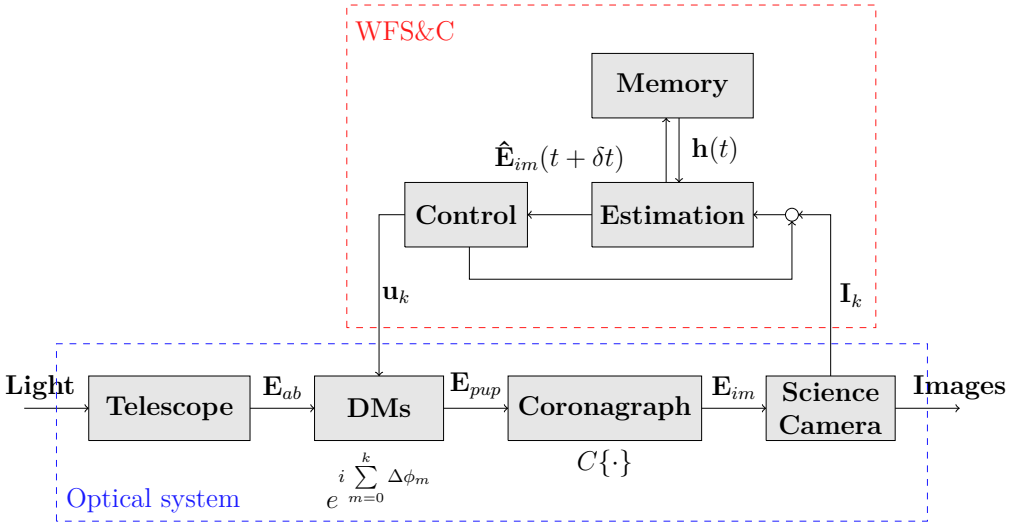

Figure 5: Block diagram of the implementation of the predictive step in the closed-loop.

4.2 Training Set

We derive in the following subsections the expression of the regressive filter **F** and explain how to find its coefficients. Without loss of generality, we consider that the value to predict is measured the history vector and all that all components in the history vector are real.

The available wavefront coefficients at time t are stored in a $n \times m$ history vector $\mathbf{h}(t)$, which is composed of the n last measurements of m different quantities

$$\mathbf{h}(t) = \begin{bmatrix} \tilde{w}_0(t) \\ \vdots \\ \tilde{w}_{m-1}(t) \\ \tilde{w}_0(t-dt) \\ \vdots \\ \tilde{w}_{m-1}(t-dt) \\ \vdots \\ \tilde{w}_{m-1}(t-(n-1)dt) \end{bmatrix} \tag{16}$$

The construction of successive history vectors is shown in Appendix **??**.

We want to train a linear filter $\mathbf{f}_i$ such that the predicted value of the wavefront i at an ulterior time is a linear sum of past measurements at the n previous times such that

$$\hat{w}_i(t+\delta t) = \mathbf{f}_i \mathbf{h}(t) \tag{17}$$

With $\mathbf{f}_i = [a^i_{0,0},\ a^i_{1,0},\ \cdots,\ a^i_{m-1,n-1}]$ the 1 by $n \times m$ vector that matches a coefficient $a^i_{j,k}$ to the j^{th} measurement of the history vector at the k^{th} time.

The filter is chosen such that it minimizes the average mean squared error, that is to say the average distance between the estimated and real value

$$\min_{\mathbf{f}_i} \langle\ || \underbrace{\hat{w}_i(t+\delta t)}_{\mathbf{f}_i \mathbf{h}(t)} - w_i(t+\delta t)||_2^2\ \rangle_T \tag{18}$$

Assuming that measurement errors $\tilde{w}_i - w_i$ are temporally uncorrelated, replacing the actual future wavefront values w_i (unknown) by the measured values yields the same optimal linear filter:

$$\min_{\mathbf{f}_i} \langle\ ||\hat{w}_i(t+\delta t) - \tilde{w}_i(t+\delta t)||_2^2\ \rangle_T \tag{19}$$

We want to train a filter based on previous measurements contained in the $n \times m$ by l data matrix

$$\mathbf{D} = \begin{bmatrix} | & | & & | \\ \mathbf{h}(t) & \mathbf{h}(t-dt) & \cdots & \mathbf{h}(t-(l-1)dt) \\ | & | & & | \end{bmatrix} \tag{20}$$

which is a horizontal concatenation of the last l history vectors, and the 1 by l a posteriori vector

$$\tilde{\mathbf{p}}_i = [\tilde{w}_i(t+\delta t),\ \tilde{w}_i(t-dt+\delta t),\ \cdots,\ \tilde{w}_i(t-(l-1)dt+\delta t)] \tag{21}$$

comprised of measured values of the i^{th} wavefront.

By averaging over a *sufficient* number of predictions, and considering that each one of them is equally weighted, we rewrite Eq. (19) in matrix form as

$$\min_{\mathbf{f}_i} ||\mathbf{f}_i \mathbf{D} - \tilde{\mathbf{p}}_i||_2^2 = \mathbf{J}(\mathbf{f}_i) \tag{22}$$

By taking the transpose, we obtain the classical least squares solution:

$$\min_{\mathbf{f}_i^T} ||\mathbf{D}^T \mathbf{f}_i^T - \tilde{\mathbf{p}}_i^T||_2^2 = \mathbf{J}(\mathbf{f}_i^T) \tag{23}$$

By setting the derivative of $\mathbf{J}(\mathbf{f}_i^T)$ to zero at the optimal filter, we have:

$$\begin{aligned}\frac{\partial \mathbf{J}(\mathbf{f}_i^T)}{\partial(\mathbf{f}_i^T)} = \frac{\partial(\mathbf{f}_i\mathbf{D}\mathbf{D}^T\mathbf{f}_i^T - \mathbf{f}_i\mathbf{D}\tilde{\mathbf{p}}_i^T - \tilde{\mathbf{p}}_i\mathbf{D}^T\mathbf{f}_i^T + \tilde{\mathbf{p}}_i\tilde{\mathbf{p}}_i^T)}{\partial(\mathbf{f}_i^T)} &= \mathbf{0} \\ \Leftrightarrow -2\mathbf{D}\tilde{\mathbf{p}}_i^T + 2\mathbf{D}\mathbf{D}^T\mathbf{f}_i^T &= \mathbf{0} \\ \Leftrightarrow \mathbf{f}_i^T = \underbrace{(\mathbf{D}\mathbf{D}^T)^{-1}\mathbf{D}}_{(\mathbf{D}^T)^+}\tilde{\mathbf{p}}_i^T\end{aligned}$$

We recognize the Moore-Penrose invert of $\mathbf{D}^T$ and obtain $\mathbf{f}_i$ by taking the transpose

$$\mathbf{f}_i = ((\mathbf{D}^T)^+\tilde{\mathbf{p}}_i^T)^T \tag{24}$$

4.3 Singular Value Decomposition of the Data Matrix

Following usual notations,

$$\mathbf{D}^T = \mathbf{U}\mathbf{\Sigma}\mathbf{V}^T \tag{25}$$

is the Singular Value Decomposition (SVD) of $\mathbf{D}^T$. $\mathbf{U}$ and $\mathbf{V}^T$ are respectively the $\mathbb{R}^{l\times l}$ and $\mathbb{R}^{nm\times nm}$ matrices of orthogonal vectors, and $\mathbf{\Sigma} \in \mathbb{R}^{l\times nm}$ the matrix composed of singular values on the diagonal. Because $\mathbf{U}$ and $\mathbf{V}^T$ are orthogonal, we have

$$(\mathbf{D}^T)^+ = \mathbf{V}\mathbf{\Sigma}^+\mathbf{U}^T \tag{26}$$

that we plug into Eq. (24)

$$\begin{aligned}\mathbf{f}_i &= (\mathbf{V}\mathbf{\Sigma}^+\mathbf{U}^T\tilde{\mathbf{p}}_i^T)^T \\ \Leftrightarrow \quad \mathbf{f}_i &= \tilde{\mathbf{p}}_i\mathbf{U}(\mathbf{\Sigma}^+)^T\mathbf{V}^T\end{aligned} \tag{27}$$

The predicted value is then

$$\hat{w}_i(t+\delta t) = \mathbf{f}_i\mathbf{h}(t) = \tilde{\mathbf{p}}_i\mathbf{U}(\mathbf{\Sigma}^+)^T\mathbf{V}^T\mathbf{h}(t) \tag{28}$$

We see in Eq. (28) that the estimate is indeed a linear combination of past measurements.

4.4 Tikhonov Regularization

The cost function Eq. (23) can also include a *regularization term* that minimizes the ℓ_2-norm of the filter matrix such that the new cost function is

$$\min_{\mathbf{f}_i^T} ||\mathbf{D}^T\mathbf{f}_i^T - \tilde{\mathbf{p}}_i^T||_2^2 + \lambda||\mathbf{f}_i||_2^2 = \mathbf{J}_R(\mathbf{f}_i^T) \tag{29}$$

with $\lambda > 0$ the regularization parameter that must be adaptated to the noise level of $\tilde{\mathbf{p}}_i^T$. Such a regularization allows to transform an ill-posed problem into a well-posed one. By introducing a term that reduces the norm of $\mathbf{f}_i$, the filter also have a better conditionning. The regularized filter then becomes

$$\mathbf{f}_i = ((\mathbf{D}_R^T)^+\tilde{\mathbf{p}}_{i_R}^T)^T \tag{30}$$

where $\mathbf{D}_R$ is the data matrix horizontally appended with the $n \times m$ identity matrix and $\tilde{\mathbf{p}}_{i_R}$ the a posteriori vector appended with $n \times m$ zeros.

4.5 Extension to Multivariate Prediction

One of the appeals of EOFs is that the only computationnaly intensive part in the SVD, which is a function of the data matrix only and also independant of the variable to be estimated. Thus, it is easy to extend Eq. (28) to predict all m values with very little computational effort. We plug other a posteriori values in an a posteriori matrix $\tilde{\mathbf{P}}$ to derive the filter to predict all m values that are measured in the history vector

$$\hat{\mathbf{w}}(t+\delta t) = \begin{bmatrix} \hat{w}_0(t+\delta t) \\ \vdots \\ \hat{w}_{m-1}(t+\delta t) \end{bmatrix} = \mathbf{F}\mathbf{h}(t) = \tilde{\mathbf{P}}\mathbf{U}(\mathbf{\Sigma}^+)^T\mathbf{V}^T\mathbf{h}(t) \tag{31}$$

With

$$\mathbf{F} = \begin{bmatrix} — & \mathbf{f}_0 & — \\ & \vdots & \\ — & \mathbf{f}_{m-1} & — \end{bmatrix} \tag{32}$$

and

$$\tilde{\mathbf{P}} = \begin{bmatrix} — & \tilde{\mathbf{p}}_0 & — \\ & \vdots & \\ — & \tilde{\mathbf{p}}_{m-1} & — \end{bmatrix} \tag{33}$$

the m by $n \times m$ filter matrix and the m by l a posteriori matrices for complete estimation, respectively.

4.6 Filter Update

As time passes, the speckles are drifting, making the history vectors in the data matrix less and less relevant because they were representative of an old state of the electric field. For that reason, it is crucial to frequently recompute the filter with actualized data.

For that purpose, the data matrix is periodically rebuilt with the latest history vectors, following a process described in Appendix C. The same operation is applied to the a posteriori matrix. In a perfect world, the filter would be computed at every iteration. Nevertheless, the SVD is costly and this is not ideal for implementation. We have to make a tradeoff between:

- The number of coefficients in the data matrix and a posteriori matrix. The more history vectors l we train our filter with, the more we will reduce the noise, but if we take too many, we have a risk of overfitting the data and training the filter with data that are *very different* from the current state. On the contrary, if we set l too small, the current estimate will be too sensitive to the current state and the noise won't be mitigated.

- The window for recomputing the filter. The more often we compute $\mathbf{F}$, the more accurate our prediction will be, but we don't need to recompute it at *every step* and we need to how long the filter provides *good* estimates before having to recompute it.

- The number of time measurements n in history vectors. The estimate being a linear combination of the n previous measurements, we have to gauge the window of our autoregression in order to take into account the *right amount* of previous states in the estimation of the next one.

- The Tikhonov regularization of the filter. It helps improving the conditioning of the problem but significantly increases the number of variables in the SVD.

All of these issues are nontrivial to tune and their choice will be critical in the efficiency of our algorithm. In Section 5, we showcase how we implemented it and how we are planning to improve it in preparation of an article.

5 Results

The algorithm is implemented in Python on both the testbed and its simulation replica. The coronagraph and optical system of the space telescope are modeled using the High Contrast Imaging for Python (HciPy) library [5]. Both cases are as close a representation of a space telescope as you would get, and the goal ultimately is to determine if the EOFs should be implemented on one of them.

The filter is trained on the l previous history vectors, each containing the n time steps, and we aim at estimating the next wavefront, thus $\delta t = dt$. We measure and estimate every component in the pixel grid of size N_{pix} in two dimensions, so $m = {N_{pix}}^2$.

The most criteria here is the contrast at the image camera plane. Indeed, we are using EOFs for dark hole maintenance, *i.e.* we have reached an *important* contrast and want to make sure it does not decrease.

5.1 Preliminary Tests

First, we showcase the preliminary tests performed to see whether the filter was working. Let's call the number of samples needed before the filter is renewed the *window* of the filter update.

Comparison of the estimation with and without filter update Let's consider a non-physical model and see how the filter behaves. Observe that we have to wait before having the first estimate on Fig. 6 : it is the training step of the filter. Without filter update, the estimated value diverges rapidly from measured value in the presence of drift. We then recompute the filter every 40 samples, which produces jumps in the estimate in the Fig. (6b). If we recompute it every 5 samples, the estimated value becomes conform to the measured value, see Fig. (6c). We need to periodically recompute the filter in presence of drift to avoid it from being outdated.

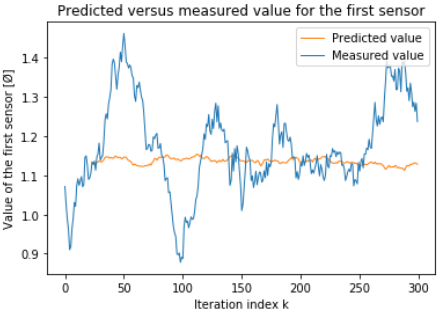

(a) No moving average.

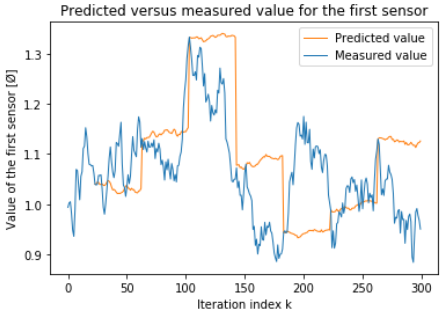

(b) With window of 40 samples.

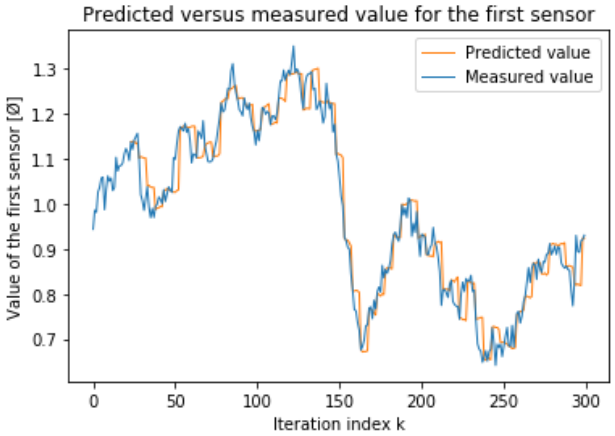

(c) With window of 5 samples.

Figure 6: Estimation and measurement of the first pixel without (top left) and with (top right) moving average. Value of the pixel in arbitrary units is shown. Estimation with small window is showed to provide much better results on the bottom.

Time series of reconstruction error with filter update We can also study at the time series of the error and observe that it diverges more and more from the a posteriori measured value the more we wait to recompute the filter, Fig. (7).

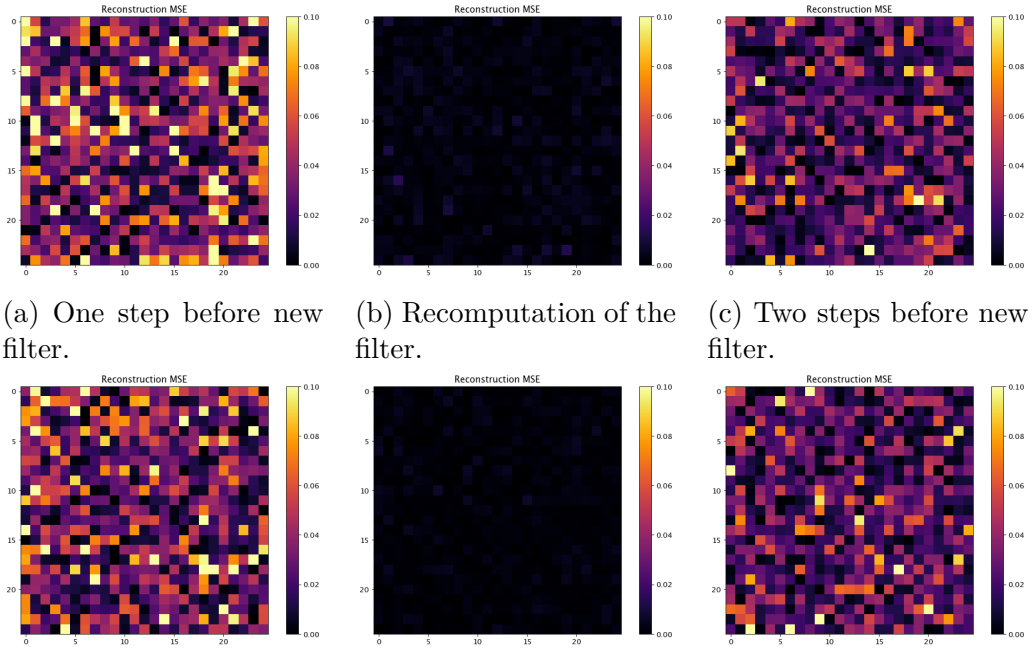

(a) One step before new filter.

(b) Recomputation of the filter.

(c) Two steps before new filter.

(d) One step before new filter.

(e) Recomputation of the filter.

(f) Two steps before new filter.

Figure 7: MSE on the pixel grid. Filter is recomputed every 3 iterations, the darker the figure, the smaller the error. Note that the scale is the same for all the plots.

Note that the results are coherent because we find the smallest error when we recomputed $\mathbf{F}$ recently, and the error gets smaller as the window gets smaller.

Speckle field intensity with phase drift Let's now examine a more physically accurate model where we simulate *strong* speckles on the science camera and add a random walk on their phase. We estimate the intensity of the speckles on all pixels of the science camera and see that we have a high reconstruction fidelity, Fig. (8)

If we study the MSE, we can see that it is sign good prediction results on Fig. (9).

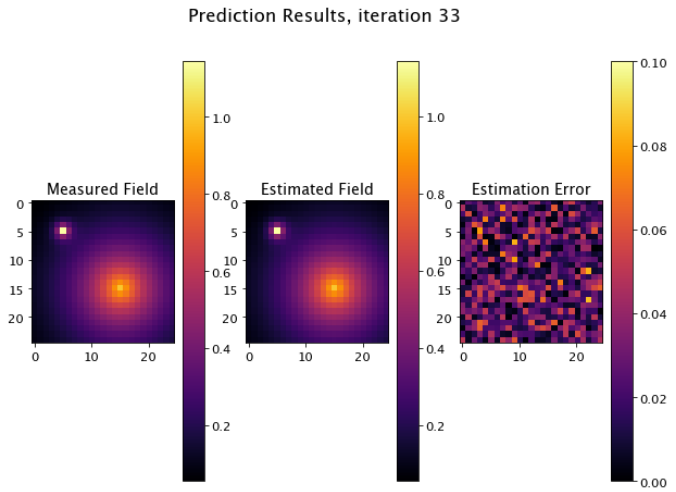

Figure 8: Comparison of estimation and measurement of the speckles intensity, reconstruction error is about 4%.

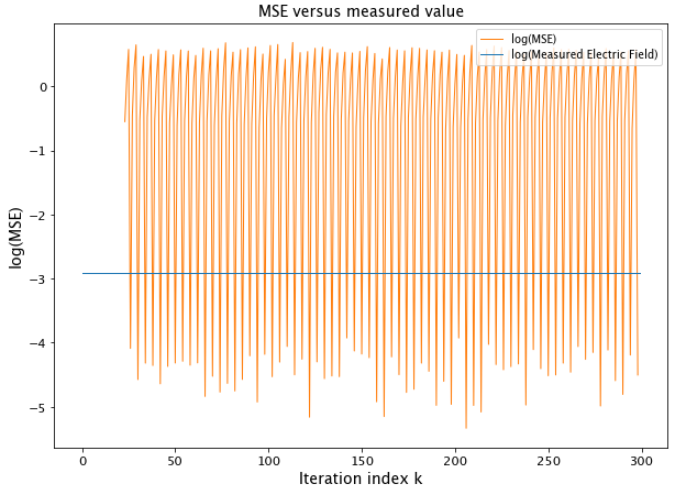

Figure 9: MSE for speckles estimation. The filter update window is 4.

Contrast reduction with pairwise estimation and stroke minimization The goal now is to see how the algorithm behaves when implemented

as part of the control loop.

We use HciPy to simulate how the control law for DMs actuation is iteratively computed. After a sufficient number of iterations, it resembles Fig. (13d) and reaches 10^{-9}.

In the next subsection, we explain how we replaced Pairwise estimation with a mix of Pairwise and EOFs and characterize the performances of the algorithm in *simulation*. Currently, the team's testbed reaches 10^{-7} in contrast and is one of the most advanced in the world. The actual space telescopes are expected to reach 10^{-10} around 2030.

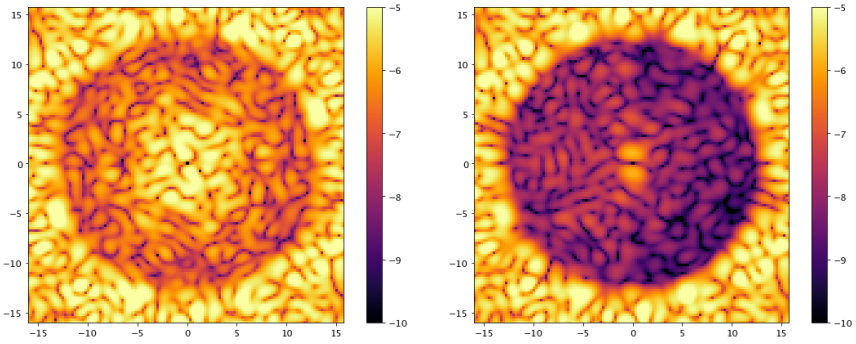

(a) Contrast after 2 steps.

(b) Contrast after 6 steps.

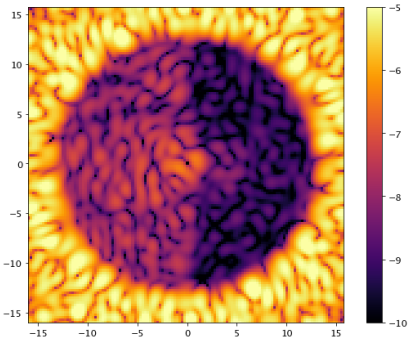

(c) Contrast after 9 steps.

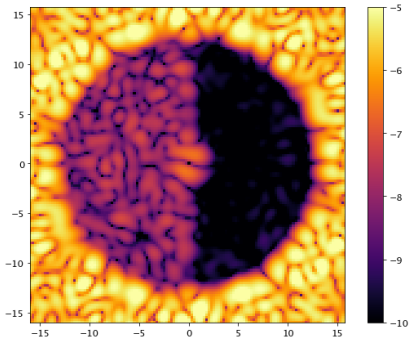

(d) Contrast after 12 steps.

Figure 10: Log-contrast on the science camera. Simulations ran on HciPy with Pairwise estimator and stroke minimization. Contrast goes from 10^{-5} to 10^{-9} in only 12 iterations.

5.2 Validation in Simulation

Now that we know that the algorithm works in very simple cases, we show the results obtained using the testbed simulator. This task was difficult because I had to get accommodated to a big project comprised of hundreds of sophisticated lines of code, on which a lot of people are simultaneously working.

We use 2 DMs and a symmetrical dual-sided dark hole. We reach the dark hole before periodically using EOFs and Pairwise estimation.

Contrast and intensity plots during dark hole maintenance In Fig. 11, we show the contrast during the dark hole maintenance step. Every few iterations, we use a batch of Pairwise estimation to compute the real electric field on the image camera plane. On the top plots, the green curve is the one we're interested in - the other ones serve to compute diagnostics. We show that the contrast stays on the order of 10^{-8} with 3 steps of EOFs followed by 3 steps of Pairwise. The bottom pictures show how deep a contrast we reach in intensity.

DMs actuation update during dark hole maintenance To make sure we are maintaining the dark hole, we can look whether the DMs acuation is *small*, which we can see is the case on Fig. 12.

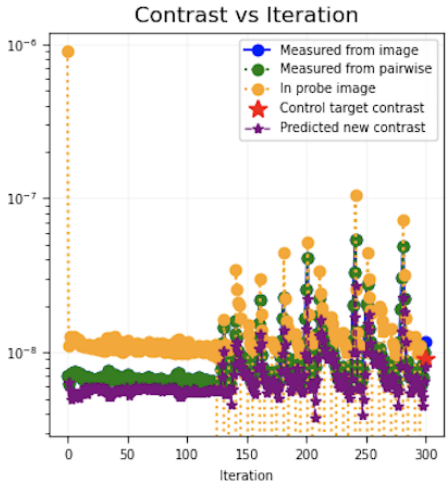

(a) Contrast with 5 steps of Pairwise estimator - 5 steps of EOFs.

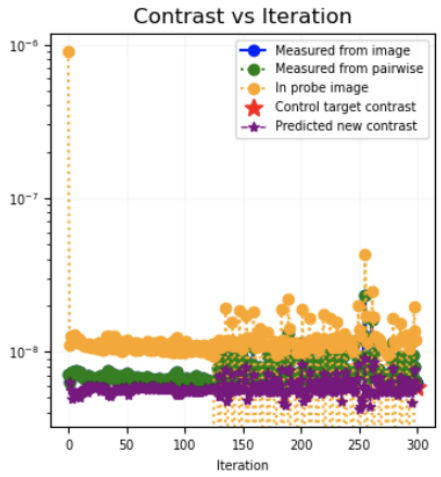

(b) Contrast with 3 steps of Pairwise estimator - 3 steps of EOFs.

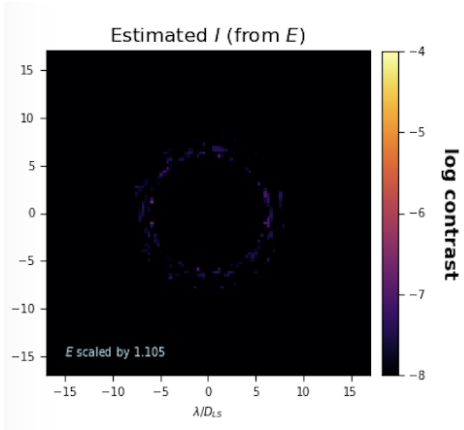

(c) Image with 5 steps of Pairwise estimator - 5 steps of EOFs.

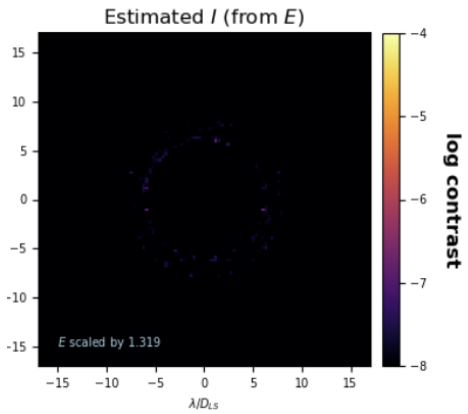

(d) Image with 3 steps of Pairwise estimator - 3 steps of EOFs.

Figure 11: Log-contrast and intensity on the science camera in simulation. Ran on the testbed using both Pairwise estimator and EOFs. Contrast is much stable in the second case.

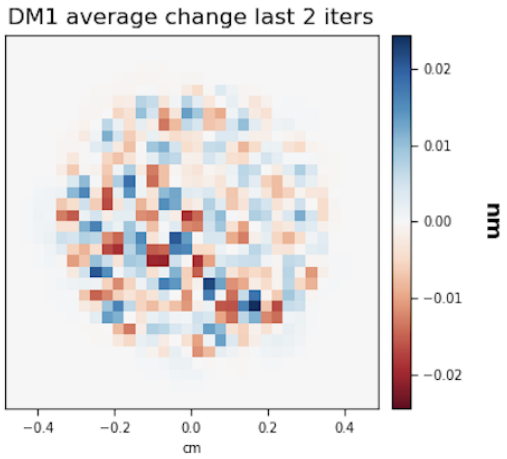

Figure 12: DM1 average update when using the correction step on EOFs prediction. Similar results can be seen on DM2.

5.3 Validation in Experimentation

After the preliminary tests and the validation in simulation, the final test was the validation on the testbed. Historically, it has always been a challenge to implement a new algorithm on it because it has so many variables - it does not behave the same way depending on the outside humidity for instance. Furthermore, I had to do it remotely from France so I was not surrounded by the team at all times like it was the case in Baltimore, and I had to work taking into account the difference in time zones.

It is a thing to develop the maths of a system and to simulate its behavior but it's a completely different order to actually make it work in practice. Thanks to the team, this is exactly what we've done. After an extensive work on the HciPy package, version control tools like Git, Python interfaces like PyCharm, having to create my own module as well as managing paths or classes issues we were finally able to make it work and these are the results.

Contrast and intensity plots during dark hole maintenance We can see on Fig. 13 that the experimentation results are very close to those in simulation which was the ultimate goal of the internship. Filter is trained on 100 vectors each containing the 5 previous measurements. We expect that we need to augment the size of the training set like in simulation and are now evaluating which parameter values are the most suitable in our case.

We already achieved a very convincing contrast while ameliorating speed by a factor 5 on a *medium-sized* dark hole - and is expected to go higher for bigger dark holes. It is also very important to notice that with the pairwise estimator, we anticipate to send probes through the optical system to estimate images, making it unusable for exoplanets observations while it is doing so. In our case, we have 4 probes that we need to add then subtract, making it 8 image exposure times where we cannot use the telecope to characterize planets. So the *overall* time gain is even greater than this, and this is a huge improvement over current methods.

Discussions on further implementation The algorithm now successfully runs on the testbed and we expect to make many more tests using different parameters. We aim at training the filter on a much more consequent training set to identify a good compromise between noise mitigation and overfitting. While the filter was unregularized because we were not able to find a parameter that did not cause the filter to completely diverge, we

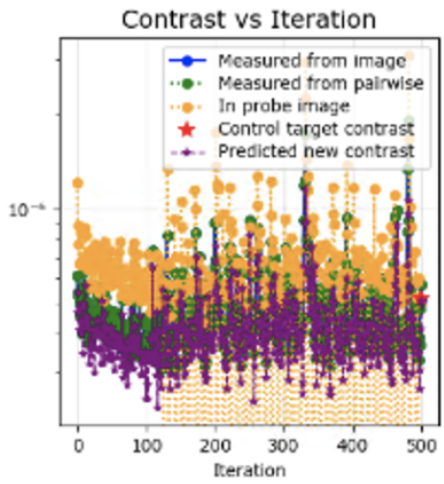

(a) Contrast with 5 steps of Pairwise estimator - 5 steps of EOFs.

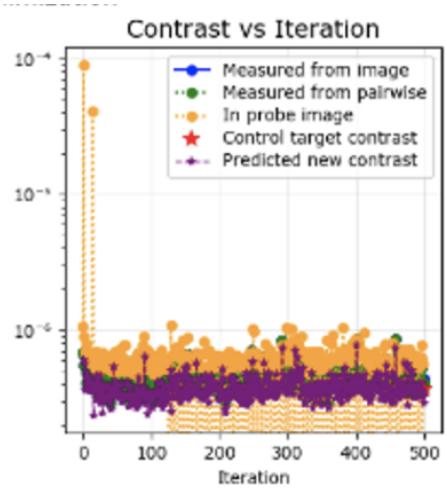

(b) Contrast with 3 steps of Pairwise estimator - 3 steps of EOFs.

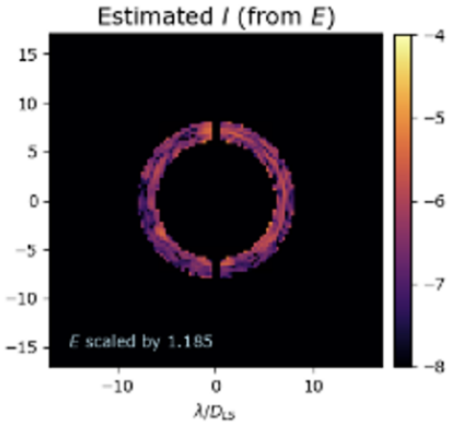

(c) Image with 5 steps of Pairwise estimator - 5 steps of EOFs.

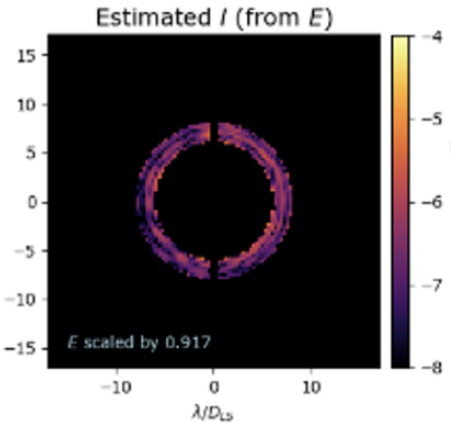

(d) Image with 3 steps of Pairwise estimator - 3 steps of EOFs.

Figure 13: Log-contrast and intensity on the science camera in experimentation. Ran on the testbed using both Pairwise estimator and EOFs. Contrast is much stable in the second case.

fully expect that a regularization would reduce the contrast even more and this is a lead we will explore. Now that the algorithm is integrated in a package, it could also be tested on some of the world's best testbeds, which the laboratory has been working closely with. Finally, it could be intagrated into an open-source library because high contrast imaging has a strong culture of sharing ressources.

6 Conclusion

This internship has been the opportunity to rigorously inspect the WFS&C landscape and identify loopholes in it. We recognized that current estimation algorithms do not account for previous photons counts on the science camera, losing a lot of information in the process. I implemented a promising predictive algorithm based on EOFs, which considers the history of speckles to enhance existing state-of-the art methods. We confirmed that it successfully estimates the electric field and it has been validated in both simulation and experimentation.

The algorithm is shown to keep a very stable level of contrast around 10^{-8} while outperforming current methods speed by a factor of five - which could go even higher if we account for larger dark zones. It is currently being evaluated to see how well it performs with an extensive parameters tuning in preparation of an article. It could expand astrophysics open-source library HciPy and be deployed on some contributors' High Contrast Imaging testbeds, for instance at Princeton University and the Jet Propulsion Laboratory.

Future space telescopes, like the James Webb Space Telescope, cost $2bn a year in maintenance and operating cost. It takes around an hour to see an exoplanet, and a week to characterize its specter. For that reason, predictive algorithms and the tremendous improvements in observation time they bring are expected to be integral part of next generations WFS&C algorithms. We hope to someday see part of the work done in this internship embarked on space.

Appendix

A Matrix to Vector Representation

The rows of the matrix are vertically concatenated to form a vector. This representation is particularly useful because it allows us to rewrite the problem with a Jacobian matrix. The numerical implementations occur on the vector, which is then reshaped to plot the electric field or its intensity on the grid of pixels of the science camera.

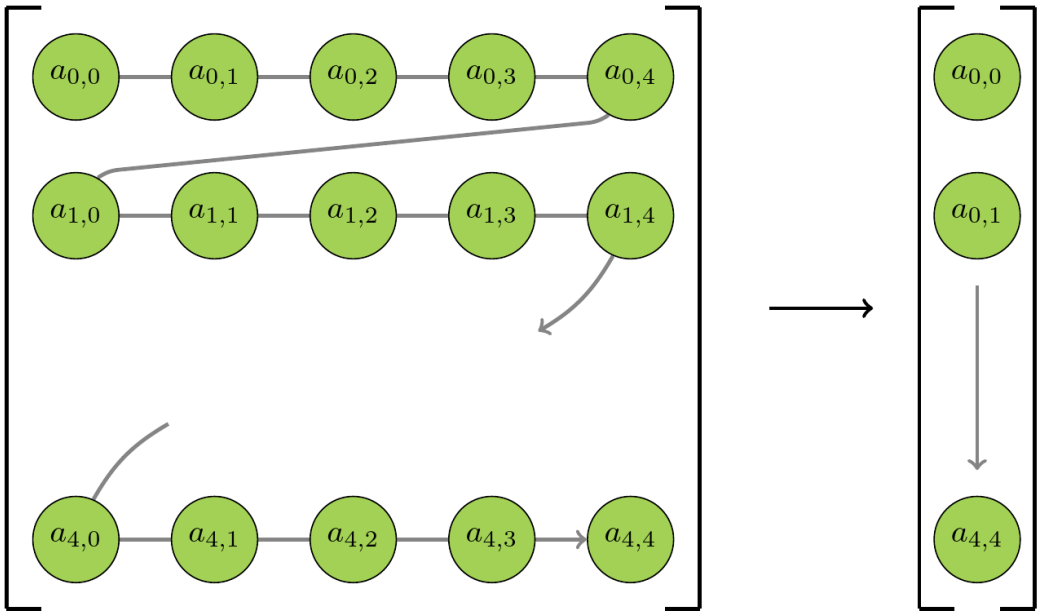

Figure 14: Transformation of a 5×5 matrix into a 25×1 vector.

B Construction of the History Vector

Each history vector discards the measurements available at the last time step and replace them with newly acquired data. The new data is added at the top and the previous vector is shifted to the bottom. In practice, this is also how they are implemented, we update a list of history vectors and the newest addition to that list is the previous array shifted to the bottom to which we add the new measurements at the top.

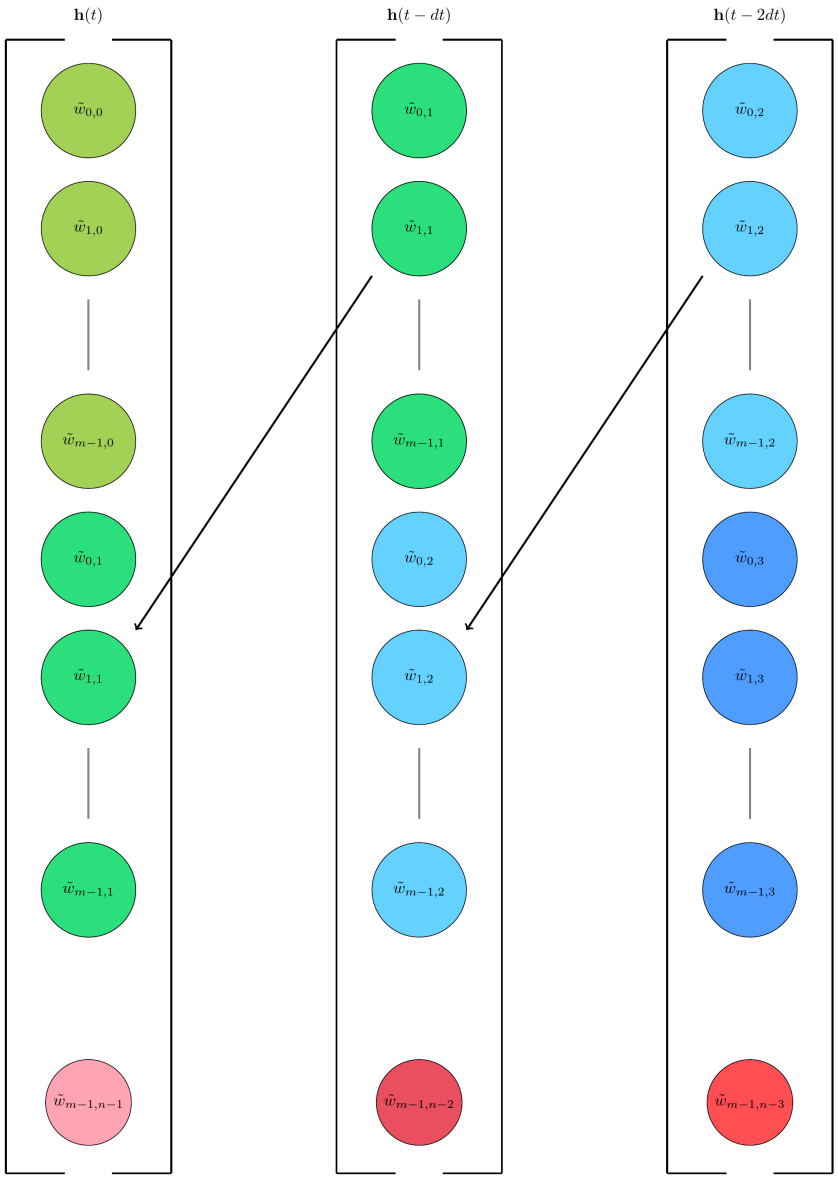

Figure 15: Construction of the history vectors.

C Filter Update

The periodic recomputation of the filter implies update of the data matrix. The example is given in the case where we recompute the filter every two time steps. The data matrix is shifted two notches to the left to incorporate new history vectors. This is particularly useful because as time goes, the oldest

samples become less and less relevant and are no longer bringing information for prediction of future states.

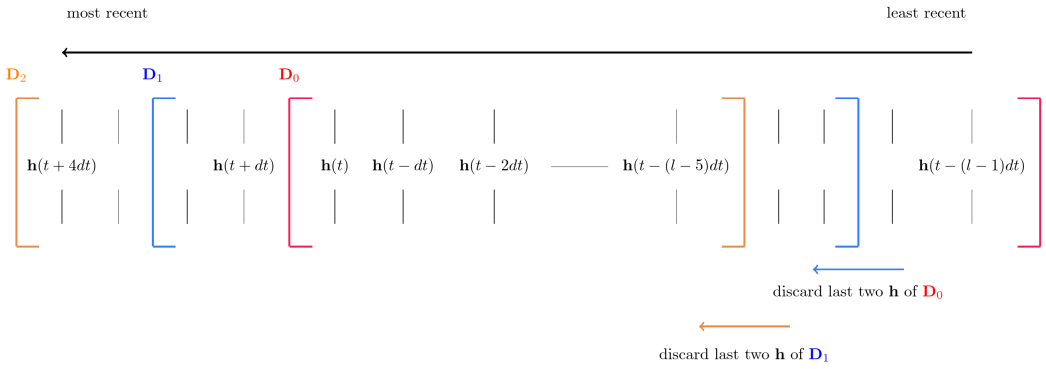

Figure 16: Rolling of data matrices for filter update.

Remark. *The a posteriori matrix undergoes a similar process.*

References

[1] Amir Give'on. The electric field conjugation - a unified formalism for wavefront correction algorithms. In *Frontiers in Optics 2009/Laser Science XXV/Fall 2009 OSA Optics & Photonics Technical Digest*, page AOWA3. Optical Society of America, 2009.

[2] Tyler D. Groff, A. J. Eldorado Riggs, Brian Kern, and N. Jeremy Kasdin. Methods and limitations of focal plane sensing, estimation, and control in high-contrast imaging. *Journal of Astronomical Telescopes, Instruments, and Systems*, 2(1):1 – 15, 2015.

[3] Olivier Guyon and Jared Males. Adaptive optics predictive control with empirical orthogonal functions (eofs), 2017.

[4] Leonid Pogorelyuk, N. Jeremy Kasdin, and Clarence W. Rowley. Reduced order estimation of the speckle electric field history for space-based coronagraphs. *The Astrophysical Journal*, 881(2):126, Aug 2019.

[5] Emiel H. Por, Sebastiaan Y. Haffert, Vikram M. Radhakrishnan, David S. Doelman, Maaike van Kooten, and Steven P. Bos. High Contrast Imaging for Python (HCIPy): an open-source adaptive optics and coronagraph simulator. In Laird M. Close, Laura Schreiber, and Dirk Schmidt, editors, *Adaptive Optics Systems VI*, volume 10703, pages 1112 – 1125. International Society for Optics and Photonics, SPIE, 2018.

[6] L. Pueyo, C. Stark, R. Juanola-Parramon, N. Zimmerman, M. Bolcar, A. Roberge, G. Arney, G. Ruane, A. J. Riggs, R. Belikov, D. Sirbu, D. Redding, R. Soummer, I. Laginja, and S. Will. The LUVOIR Extreme Coronagraph for Living Planetary Systems (ECLIPS) I: searching and characterizing exoplanetary gems. In Stuart B. Shaklan, editor, *Techniques and Instrumentation for Detection of Exoplanets IX*, volume 11117, pages 37 – 65. International Society for Optics and Photonics, SPIE, 2019.

[7] Laurent Pueyo, Vanessa Bailey, Matthew Bolcar, Laura Coyle, Lee Feinberg, Tyler Groff, Olivier Guyon, Jeffrey Jewell, Jeremy Kasdin, Scott Knight, Dimitri Mawet, Johan Mazoyer, Bertrand Mennesson, Marshall Perrin, David Redding, AJ Riggs, Garreth Ruane, Remi Soummer, Christopher Stark, Scott Will, and Neil Zimmerman. Wavefront Sensing and Control technologies for Exo-Earth imaging. volume 51, page 215, Sep 2019.

[8] Laurent Pueyo, Jason Kay, N. Jeremy Kasdin, Tyler Groff, Michael McElwain, Amir Give'on, and Ruslan Belikov. Optimal dark hole generation via two deformable mirrors with stroke minimization. *Appl. Opt.*, 48(32):6296–6312, Nov 2009.

Acknowledgements

First of all, I'd like to thank Laurent and Colin for trusting me and inviting me to Baltimore. Laurent, you've been a great mentor both on and off work and taught me a lot about how to think. I'm very grateful I got the opportunity to work with you. Rémi, thank you for becoming my unofficial tutor once I started working on the testbed and making yourself available - even at odd hours - once I started working remotely. Your problem solving skills helped me decompose problems in a much smarter way. I'd like to thank Marshall & Jamie for all the discussions on the software, the HiCAT Python environment and Git. Scott, thank you for taking the time to explain how to interpret statistical models and best of luck at Goddard. Iva, thank you for bringing my suitcase back and welcome to Marseille! Jules, I had a great time cracking jokes with you, best of luck for your transition to California - I'm certain it'll be a great fit for you! Overall, I'd like to express my deepest gratitude to the whole Space Telescope Science Institute team for providing a warm and friendly work environment, as well as helping me solve the very complex problems I might have encountered. This goes to Kelsie, Greg, Keira, Susan, Peter, Heather, Evelyn, Tom, Yinzi, Sam as well as every people outside of the Makidon lab I've had the chance to interact with.

To Kevin, Xandi, Kelechi and Gabe, thank you for having me as a roommate, and introducing me to many Hopkins students. I had a great year because of you, and I definitely hope we'll see each other again when the time is right! To all my friends at the Department of Physics and Astronomy, in particular Erwin, Anubhav and Yasuo - we never got to play soccer in the end but I hope you're well. Last but not least, I'd like to address a special thank you to Ms. Durieu for putting me in contact with Laurent. I wouldn't have had this internship it weren't for you. All your teachings were put to great use!